Theor Chem Acc (2002) 108:103–112
DOI 10.1007/s00214-002-0361-y

Theoretical
Chemistry Accounts

Regular article

Recombination of *tert*-butyl radicals: the role of weak van der Waals interactions

Marek Naroznik[1], **Jan Niedzielski**[2]

[1]Chemical–Mathematical Department, University of Podlasie, 08-110 Siedlce, Poland
[2]Chemistry Department, Warsaw University, 02-089 Warsaw, Poland

Received: 2 October 2000 / Accepted: 2 May 2002 / Published online: 7 August 2002

Abstract. A mechanism for the recombination of *tert*-butyl radicals is postulated to involve the loosely bonded intermediates *tert*-$C_4H_9\cdots$*tert*-C_4H_9. Three processes contribute to the overall recombination rate constant: *tert*-C_4H_9 + *tert*-C_4H $\leftrightarrow$ *tert*-$C_4H_9\cdots$*tert*-C_4H_9 characterized by the equilibrium constant K_1 and *tert*-$C_4H_9\cdots$*tert*-$C_4H_9 \rightarrow C_8H_{18}{}^*$ characterized by the rate constant k_2, $k_{\mathrm{rec},\infty}(T) \approx K_1k_2$. This recombination rate constant exhibits a negative temperature dependence and is proportional to $T^{-3/2}$. The agreement with experiment is very good.

Key words: *tert*-Butyl radical recombination

1 Introduction

Since radical recombination reactions play so important a role in combustion and atmospheric processes many experimental and theoretical studies have been devoted to this subject.

The statistical adiabatic channel model (SACM) [1] provided a link to the molecular and radical parameters. This theory, for many reasons, turned out to be very convenient. For instance, it allowed the rate constant of unimolecular dissociation to be calculated precisely and, hence, the recombination rate constant by correlating the reactant and product states. The variational transition-state theory [2] was postulated in many different versions: to study the CH_3 + H system by Hase and coworkers [3, 4] and by Aubanel and Wardlaw [5], and to study the CH_3 + CH_3 system by Wardlaw and Marcus [6]. This theory was further developed and offered a precise description of the effect of the angular potential [7, 8, 9, 10, 11, 12].

Other original approaches include the classical trajectories calculations of Hu and Hase [13] and the improved version of the Gorin model [14, 15, 16]. The recent work by Pacey [17] expressed the rocking force constants and the length of the forming bond, R, as a function of the potential energy along the reaction coordinate instead of expressing the potential energy as a function of R and angles.

Our earlier work was concerned with a mechanism of radical recombination [18, 19, 20, 21]. We emphasize the importance of weak van der Waals interaction in the process of recombination. Benson [15] and Clary [22] earlier studied the problem of weak interactions. In our works, we include some aspects of dynamics of the system by solving the pertinent form of the Schrödinger equation and using the available ab initio calculations.

We have previously established [20] that in the system CH_3 + CH_3 at a distance between the centres of mass of about 3.8–4.0 Å the energy of the weak interactions shows a shallow minimum. If so, the loosely bonded states in the form of the physichemical $CH_3\cdots CH_3$ compounds occur. Apart from the attractive force, the centrifugal repulsive force resulting from the orbital motion quantized with the l number has to be reckoned with. As l increases the potential-energy minimum becomes shallower and vanishes completely at some critical value for $l = \langle l_{\mathrm{lim}}\rangle$. The $CH_3\cdots CH_3$ compounds cannot be formed at such states.

During their short lifetime the $CH_3\cdots CH_3$ adducts undergo the rearrangement of the internal rotational energy under the action of interaction potentials that are strongly angle-dependent. The rearrangement of rotational energy to achieve the maximum overlap of unfilled radical orbitals may result in the formation of a new bond which is tantamount to the radical recombination.

On the basis of such a mechanism we have shown that at high pressures and temperatures the magnitude of the resultant recombination rate constant is practically limited by the rate of formation of short-lived $CH_3\cdots CH_3$ adducts [20]. This recombination rate constant decreases as the temperature increases. The negative temperature dependence obeys the proportionality $T^{-1/2}$. This effect can be rationalized by the enhanced contribution of large l ($l > \langle l_{\mathrm{lim}}\rangle$) at high temperatures. Consequently, the number of $CH_3\cdots CH_3$ van der Waals

---

Correspondence to: M. Naroznik

complexes decreases, and so does the rate of recombination.

To verify this mechanism, the CH_3 + H system was considered [21]. This system exhibits an energy of interaction smaller by about 1 order of magnitude and also a much smaller reduced mass than the system characteristic for the methyl radical recombination. The calculations indicate that loosely bonded $CH_3 \cdots H$ adducts that are transformed into hot CH_4^* molecules are also formed. However, the negative temperature dependence of the recombination rate constant, proportional to $T^{-1/2}$, has not been confirmed. A comparison with experimental recombination rate constants indicates that the mechanism involving weak van der Waals complexes does not predominate. Apparently, direct head-on reactant collisions contribute more to recombination. Compared with the recombination of methyl radicals, the reactant interaction energy is too small.

To conclude, we have shown that the recombination of small hydrocarbon radicals can be described as a multistep process. The contribution of the separate steps depends on the temperature and pressure as well as on the individual properties of the reactants. According to calculations, the energy of interaction and the reduced mass are of special importance. Thus, the *tert*-C_4H_9 + *tert*-C_4H_9 system presents an interesting case.

$$\textit{tert}\text{-}C_4H_9 + \textit{tert}\text{-}C_4H_9 \xrightarrow{k} C_8H_{18} \tag{1}$$

As will be commented on later, a potential minimum for the van der Waals interactions in this system is $D_0 = 1.11$ kcal mol^{-1}, i.e. about 3 times as much as in the recombination of methyl radicals. Also the reduced mass of the reacting *tert*-butyl radicals is much larger, by about a factor of 4. The system seems to be a good model to verify the hypothesis of the importance of interaction energy and reduced mass in the recombination.

The reaction in Eq. (1) has been studied both experimentally [23, 24, 25, 26, 27, 28] and theoretically [15, 29]. Experimental results [26] indicate that the recombination rate constant, $k_{\mathrm{rec},\infty}$, shows a marked negative temperature dependence that goes as $k_{\mathrm{rec},\infty} \sim T^{-3/2}$.

The aim of this work is to find out whether or not the mechanism involving the formation of weak van der Waals complexes can be used to describe the recombination of *tert*-butyl radicals.

2 Interactions and the bonded states of radicals

On the basis of the assumptions concerning the weakly interacting systems, the Hamiltonian for the pair of *tert*-butyl radicals can be written as

$$\hat{\mathrm{H}} = \hat{\mathrm{H}}_{\mathrm{r}} + \hat{\mathrm{H}}_J \ , \tag{2}$$

where

$$\hat{\mathrm{H}}_J = \hat{\mathrm{H}}_{\mathrm{rot}_1} + \hat{\mathrm{H}}_{\mathrm{rot}_2} + \hat{\mathrm{H}}_{\mathrm{orb}} + V \ . \tag{3}$$

The subscript J refers to the total angular momentum of the system, whereas the term $\hat{\mathrm{H}}_{\mathrm{r}}$ is the operator describing the motion of radicals along the distance r in the centre-of-mass frame. $\hat{\mathrm{H}}_{\mathrm{rot}_1}$ and $\hat{\mathrm{H}}_{\mathrm{rot}_2}$ are the operators for the intrinsic rotational energy of the respective radicals and $\hat{\mathrm{H}}_{\mathrm{orb}}$ describes the relative orbital energy. All the details concerning such operators are given in former work [18, 19]. V is the interaction potential of the radicals.

Two separate interactions contribute to the radical interaction potential:

$$V = V_{\mathrm{B}} + V_{\mathrm{NB}} \ . \tag{4}$$

The bonded interactions, V_{B}, result from the overlap of radical shells which both feature a vacancy. In the *tert*-butyl radicals, assuming the occurrence of sp^2 hybridization of the central carbon atom, the p_z orbitals are of concern. Such an overlap was thoroughly discussed for the CH_3 + CH_3 system [18]. The values for V_{B} should not differ much in both these cases. We have obtained the following form for the V_{B} potential:

$$V_{\mathrm{B}} = -A \exp\left(-\frac{Zr}{a_0}\right)[f_1(r)\cos\theta_{12} - f_2(r)\cos\theta_1\cos\theta_2]^2 \ , \tag{5}$$

where

$$f_1(r) = 1 + \frac{1}{15}a[15 + a(6 + a)] \ , \tag{6}$$

$$f_2(r) = a^2\frac{1}{5}\left[1 + a\left(1 + \frac{1}{3}a\right)\right] \tag{7}$$

and

$$a = \frac{Zr}{2a_0} \ . \tag{8}$$

$\cos\theta_1$, $\cos\theta_2$ and $\cos\theta_{12}$ are the cosines describing the mutual orientation of reactants, a_0 is the Bohr orbit, while the magnitudes for the constant parameters are $Z = 2.72$ and $A = 564.2$ kcal mol^{-1} [18].

The second type of interactions, V_{NB}, describes the attractive dispersion forces, short-range repulsive interactions and eventual multipole interactions. In one of the most widespread methods for the estimation of the potential V_{NB} the reactants are treated as semirigid objects whose interactions are given by the sum of interactions from site to site [30, 31, 32]. The sites are either "atoms" constituting a molecule or are the centres of increased electric charge density.

$$V_{\mathrm{NB}} = \sum_{ij} V_{ij}(r_{ij}) \ , \tag{9}$$

where i and j are the atoms on molecules A and B, respectively, while r_{ij} is the distance between these sites.

In the hard-sphere approximation the potential (Eq. 9) can be presented in the convenient spherically symmetrical form. For the *tert*-C_4H_9 + *tert*-C_4H_9 system the Morse function seems to be a good choice ($V_{\mathrm{NB}} = V_{\mathrm{M}}$):

$$V_{\mathrm{M}}(r) = D_0\{1 - \exp[-\beta_0(r - r_0)]\}^2 - D_0 \ , \tag{10}$$

where $D_0 = 1.11$ kcal mol^{-1}, $r_0 = 5.53$ Å and $\beta_0 = 1.41$ Å^{-1}. This function has been determined on the basis of experimental second virial coefficients for the *iso*-C_4H_{10} + *iso*-C_4H_{10} system [33, 34]. The D_0 and r_0 obtained are in perfect agreement with those reported for similar systems [32, 33].

V_B and V_{NB} for the selected r are listed in Table 1. It is clearly seen that at r > 5 Å, V_B is smaller by 2 orders of magnitude than V_{NB} even for the case of maximum *s*-type overlap of p_z orbitals (staggered geometry). Since we are mostly interested in the direct vicinity of the potential minimum, r_0, the short-range bonded interactions are entirely unimportant. Only at r < 4 Å is V_B comparable or even larger than V_{NB}.

By approximating the potential of the radical interaction to its spherically symmetric form (Eq. 10) we can use the known solutions of the Schrödinger equation [19, 20]:

$$\hat{H}_J \psi_n^{JM} = E_n(r) \psi_n^{JM} \ . \tag{11}$$

The term $E_n(r)$ represents the total energy of the rotational motion which depends on the set of quantum numbers $n \equiv \{j_1, k_1, j_2, k_2, j, l, J\}$ and the distance r [19]:

$$E_n(r) = E^{(0)}_{j_1,k_1} + E^{(0)}_{j_2,k_2} + \frac{\hbar^2}{2\mu r^2} l(l+1) + V_M(r) \ , \tag{12}$$

where

$$E^{(0)}_{j_1,k_1} = A_1 j_1(j_1+1) + (B_1 - A_1)k_1^2 \tag{13}$$

and

$$E^{(0)}_{j_2,k_2} = A_2 j_2(j_2+1) + (B_2 - A_2)k_2^2 \ . \tag{14}$$

A_1, B_1, A_2 and B_2 are the rotational constants. Assuming the sp^2 hybridization of the central carbon atom and the known geometrical parameters of the methyl groups [35], for the rotational constant of *tert*-butyl we obtain $A_1 = 7.364 \times 10^{-4}$ kcal mol^{-1}, $B_1 = 3.964 \times 10^{-4}$ kcal mol^{-1}, $A_2 = A_1$ and $B_2 = B_1$. μ stands for the reduced mass of the system. j_1 is the quantum number for the intrinsic momentum of the first radical, and k_1 is its projection on the z-axis of the system rigidly interlinked with the radical ($-j_1 < k_1 < j_1$). The same numbers marked with the subscripts 2 refer to the second radical. As already mentioned, the l number quantizes the orbital momentum of the radicals.

By taking into account the law of total momentum conservation, the wave function Ψ_n^{JM} for the system of *tert*-butyl radicals can be expressed in the form [19, 36]

$$\Psi_n^{JM} = N \sum_{m_l m_j} \left(\begin{array}{cc|c} l & j & J \\ m_l & m_j & M \end{array} \right) \times \sum_{m_1 m_2} \left(\begin{array}{cc|c} j_1 & j_2 & j \\ m_1 & m_2 & m_j \end{array} \right) D^{j_1}_{m_1,k_1} D^{j_2}_{m_2,k_2} Y_{l,m_l} \ . \tag{15}$$

m_1 is the projection of j_1 on the fixed axis z' ($-j_1 < m_1 < j_1$), while m_l is the projection of l on the fixed axis in the centre-of-mass frame. j is the superposition $|j_1 - j_2| < j < j_1 + j_2$, $m_j = m_1 + m_2 J$ quantizes the total momentum of the system and falls in the range $|l - j| < J < l + j$, while $M = m_j + m_l$ is its resultant projection on the fixed axis. $D^{j_1}_{m_1,k_1}$ is the generalized spherical function describing the rotational motion of the first radical. Analogous notation refers to the second radical. Y_{l,m_l} is a wave function, spherical harmonic, describing the orbital motion of the radicals. $\left(\begin{array}{cc|c} j_1 & j_2 & j \\ m_1 & m_2 & m_j \end{array} \right)$ are the coefficients for the expansion of the states determined by the numbers $|j,m_j>$ into the states determined by the numbers $|j_1,m_1>|j_2,m_2>$, called the Clebsch–Gordon coefficients [36]. Similarly, $\left(\begin{array}{cc|c} l & j & J \\ m_l & m_j & M \end{array} \right)$ are the coefficients for expansion of the states $|J,M>$ into the states $|j,m_j>|l,m_l>$. N is the normalization constant.

Typical $E_n(r)$ curves are shown in Fig. 1. A distinct minimum is visible that disappears at l > 225. Since a spherically symmetric interaction potential was assumed, this value is independent of the other quantum numbers, i.e. j_1, k_1, etc. The value for l_{lim}, averaged over all the states, is therefore $\langle l_{\text{lim}} \rangle = 225$. Recall that $\langle l_{\text{lim}} \rangle = 39$ for CH_3 + CH_3 [20] and $\langle l_{\text{lim}} \rangle = 13$ for CH_3 + H [21]. The difference is substantial. It results not only from the greater interaction energy in the *tert*-C_4H_9 + *tert*-C_4H_9 system but to an even higher a degree from the much larger reduced mass.

A solution of the Schrödinger equation using the full Hamiltonian (Eq. 2) indicates that the reactants form the bonded *tert*-$C_4H_9 \cdots$*tert*-C_4H_9 complex. Transformations analogous to those described in Ref. [20] give the radial form of the Schrödinger equation:

Table 1. Interaction potentials V_{NB} and V_B (kcal mol^{-1}) for the staggered geometry at selected distances for the system *tert*-C_4H_9 + *tert*-C_4H_9

r/Å	V_B	V_{NB}
4.80	−0.0331	2.4828
5.00	−0.0163	0.2608
5.20	−0.0079	−0.7203
5.50	−0.0026	−1.1079
6.66	0.0	−0.4054
7.00	0.0	−0.2618
7.33	0.0	−0.1685
7.66	0.0	−0.1074

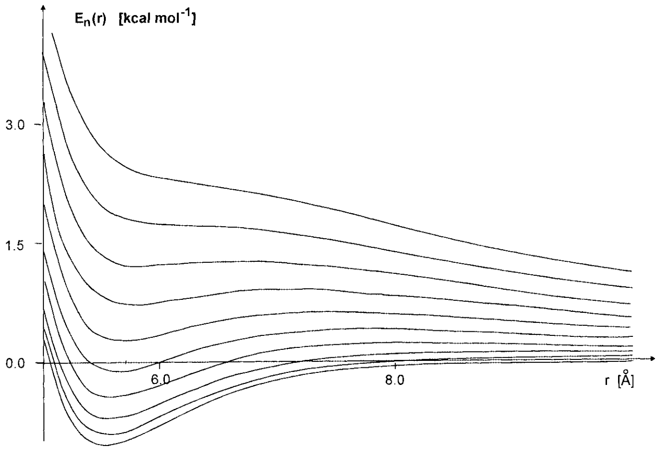

Fig. 1. Typical $E_n(r)$ potential curves. From *top* to *bottom*: third group – l = 260, 235; second group – l = 210, 185, 160, 135, 110, 85, 60, 35

$$\left(-\frac{\hbar^2}{2\mu}\frac{\mathrm{d}^2}{\mathrm{d}r^2}+E_n(r)\right)\chi_n(r)=E\chi_n(r)\ . \tag{16}$$

Equation (16) describes the relative translational motion of the reactants along the r radius under the action of the $E_n(r)$ potential. For zero orbital momentum ($l=0$) we obtain

$$\begin{aligned}&-\frac{\hbar^2}{2\mu}\frac{\mathrm{d}^2}{\mathrm{d}r^2}\chi_n(r)+\{D_0\exp[-2\beta_0(r-r_0)]-2D_0\\&\qquad\times\exp[-\beta_0(r-r_0)]\}\chi_n(r)\\&\quad=\left(E-E^{(0)}_{j_1,k_1}-E^{(0)}_{j_2,k_2}\right)\chi_n(r)\ .\end{aligned}\tag{17}$$

By substituting

$$E'=E-E^{(0)}_{j_1,k_1}-E^{(0)}_{j_2,k_2} \tag{18}$$

and

$$R=r-4.5\,\text{Å} \tag{19}$$

we obtain after simple transformations

$$\begin{aligned}&\left[\frac{\mathrm{d}^2}{\mathrm{d}R^2}-U_1\exp(-2R\beta_0)+U_2\exp(-R\beta_0)-\kappa^2\right]\chi_n(R)\\&\quad=0\ ,\end{aligned}\tag{20}$$

where

$$U_1=\frac{2\mu}{\hbar^2}D_0\exp\left[-2\beta_0(4.5\ \text{Å}-r_0)\right]\ , \tag{21}$$

$$U_2=\frac{2\mu}{\hbar^2}2D_0\exp\left[-\beta_0(4.5\ \text{Å}-r_0)\right] \tag{22}$$

and

$$\kappa^2=-\frac{2\mu}{\hbar^2}E'\ . \tag{23}$$

Solutions of Eq. (20) are known [37]. By transforming Eq. (20) into the hypergeometrical equation and using the regularity condition for the solution at $R=0$ (see the appendix in Ref. [20], we obtain the 18 energy levels shown in Fig. 2 ($j_1=0$, $j_2=0$). The approximations use the well-known formula

$$E_v=h\nu_0\left(v+\frac{1}{2}\right)-xh\nu_0\left(v+\frac{1}{2}\right)^2-D_0\ . \tag{24}$$

It is seen that the energy levels of the anharmonic oscillator shifted at the energy axis by a value D_0 are obtained, where the intrinsic frequency $h\nu_0=42.7\ \text{cm}^{-1}$, the anharmonicity coefficient $x=0.02751$ and v takes the values 0,1,...17.

We have shown that *tert*-butyl radicals at $l=0$ form the bonded states *tert*-$C_4H_9\cdots$*tert*-C_4H_9 characterized by the energy levels estimated earlier. Such states also exist, of course, at $l>0$. Accurate calculation of their energy levels requires the numerical solution of differential Eq. (16). We do not attempt to solve this problem in this work, even though we try to make some corrections that would alleviate this deficiency. This problem will be commented on later. The important point is that a classical criterion for the existence of the bonded state is assumed: the presence of a minimum on the $E_n(r)$ curve. We ignore any quantum effects that would forbid the occurrence of such states at too shallow well depth. Such effects were found insignificant for the CH_3 + CH_3 system [7].

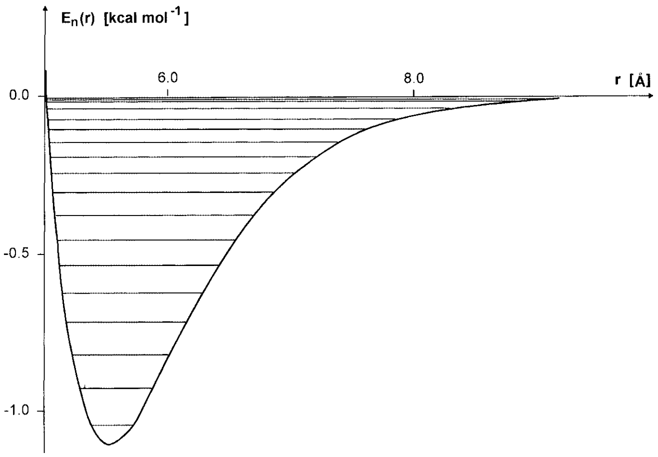

Fig. 2. $E_n(r)$ versus interradical distance for the set $n\equiv\{l=0, j_1=0, j_2=0\}$. *Horizontal lines*: allowed energy levels, E_v

3 Mechanisms and equilibria

In the analysis of the methyl recombination, three groups of the curves that describe the $E_n(r)$ potential were singled out [20]. The first-group curves exhibit a sharp decrease towards decreasing r that leads directly to recombination. The curves from the second group exhibit a distinct minimum associated with the presence of weakly bound $CH_3\cdots CH_3$ states. The minimum depth is on average 0.6 kcal mol^{-1} [18, 19, 20]. This minimum refers to the specific rotational states that include different orientations of the radicals. The energy levels for such states were estimated by solving the pertinent Schrödinger equation [19, 20]. If the simpler static approach is adopted, i.e. only one specific orientation is taken into account, such a deep minimum cannot be found [12], and, consequently, the importance of the van der Waals complexes cannot be revealed. The curves from the third group show a continuous increase as r decreases; under such conditions the $CH_3\cdots CH_3$ complexes cannot form ($l>\langle l_{\text{lim}}\rangle$). Since the j_1, j_2, k_1, k_2 and l as well as j quantum numbers are not conserved, even though J is, the internal rearrangement of the rotational energy occurs, leading to the change in the character of the $E_n(r)$ potential, including the change in the affiliation to the specific group.

The *tert*-C_4H_9 + *tert*-C_4H_9 system exhibits similar behaviour. The curves that belong to the second and third groups are shown in Fig. 1. Since we use the averaged $V_{\text{NB}}=V_{\text{M}}(r)$ potential and the V_{B} potential was not taken into account, we do not present the curves belonging to the first group. We have previously shown [18, 19, 20] that V_{B} interactions are important only at very short range, $r<4$ Å. Only over this region does V_{B}

show a sharp decrease that determines the presence of $E_n(r)$ belonging to the first group. At the ranges of interest in the *tert*-C_4H_9 + *tert*-C_4H_9 system, $r > 5$ Å, V_B is so small compared with V_{NB} that its contribution can safely be ignored. However, this approximation notwithstanding, very few curves that belong to the first group are really present affecting the occurrences in a similar way as in the case for the recombination of methyl radicals.

Thus, at the initial conditions defined by the set of n quantum numbers and under the condition $l < \langle l_{\text{lim}} \rangle$, the loosely bound *tert*-$C_4H_9 \cdots$*tert*-C_4H_9 complexes are formed as the first step with a rate constant k_1. The internal rearrangement of the rotational energy alters the character of the $E_n(r)$ curve: the transformation from the second to the first or to the third group. The physichemical *tert*-$C_4H_9 \cdots$*tert*-C_4H_9 compounds either undergo spontaneous dissociation back to the reactants with a rate constant k_{-1} or form the hot molecule of tetramethylbutane (C_8H_{18}*) with a rate constant k_2. The energy of the weak *tert*-$C_4H_9 \cdots$*tert*-C_4H_9 bond at $l > 0$ is of the order of 0.1 kcal mol^{-1}. It is comparable with an average energy $|\Delta E|$ transferred per collision. For instance, for the C_2H_6–Ar system, $\langle \Delta E \rangle$is reported to be -0.5863 ± 0.1859 kcalmol^{-1} on the basis of experimental measurements on the $CH_3 + CH_3 \rightarrow C_2H_6$ system [38] and calculations using a microcanonical variational Rice–Ramsperger–Kassel–Marcus rate constant calculation [8]. Thus, the loosely bonded compounds can decompose in collisions with a rate constant λZp, where Z is the number of collisions, p is the pressure of the bath gas and λ is the collisional efficiency [39]. Therefore, for the states characterized by $l < \langle l_{\text{lim}} \rangle$ we postulate a mechanism

$$\textit{tert}\text{-}C_4H_9 + \textit{tert}\text{-}C_4H_9 \xrightarrow{k_1} \textit{tert}\text{-}C_4H_9 \cdots \textit{tert}\text{-}C_4H_9 \ , \quad (25)$$

$$\textit{tert}\text{-}C_4H_9 \cdots \textit{tert}\text{-}C_4H_9 \xrightarrow{k_{-1}} \textit{tert}\text{-}C_4H_9 + \textit{tert}\text{-}C_4H_9 \ , \quad (26)$$

$$\textit{tert}\text{-}C_4H_9 \cdots \textit{tert}\text{-}C_4H_9 \xrightarrow{\lambda Zp} \textit{tert}\text{-}C_4H_9 + \textit{tert}\text{-}C_4H_9 \ , \quad (27)$$

$$\textit{tert}\text{-}C_4H_9 \cdots \textit{tert}\text{-}C_4H_9 \xrightarrow{k_2} C_8H_{18}^* \ , \quad (28)$$

$$C_8H_{18}^* \xrightarrow{k_{-2}} \textit{tert}\text{-}C_4H_9 \cdots \textit{tert}\text{-}C_4H_9 \ , \quad (29)$$

$$C_8H_{18}^* \xrightarrow{\omega} C_8H_{18} \ , \quad (30)$$

$$C_8H_{18}^* \xrightarrow{k_{-3}} \textit{tert}\text{-}C_4H_9 + \textit{tert}\text{-}C_4H_9 \ , \quad (31)$$

where ω is the collisional frequency. This mechanism has to be supplemented by the recombination that occurs for the states that feature $l > \langle l_{\text{lim}} \rangle$, i.e. under the conditions that preclude the formation of van der Waals adducts:

$$\textit{tert}\text{-}C_4H_9 + \textit{tert}\text{-}C_4H_9 \xrightarrow{k_1'} C_8H_{18}^* \ . \quad (32)$$

By taking into account the rate of tetramethylbutane formation, d[C_8H_{18}]/dt, and combining Eqs. (1) and (30) we obtain

$$k[\textit{tert} - C_4H_9][\textit{tert} - C_4H_9] = \omega\left[C_8H_{18}^*\right] \ . \quad (33)$$

Since both *tert*-$C_4H_9 \cdots$*tert*-C_4H_9 states and hot C_8H_{18}* molecules are unstable, the stationary-state approximation can be used to describe such species. Hence, the concentration for excited tetramethylbutane, [C_8H_{18}*], can be estimated. Taking into account Eq. (33) and an additional condition valid at high pressures, $\omega \gg k_{-3}$ [39, 40] (as well as $\omega \gg k_{-2}$), a mechanism involving Eqs. (25), (26), (27), (28), (29), (30), (31) and (32) gives for the rate constant k (Eq. 1)

$$k = \frac{1}{1 + (k_{-1} + \lambda Zp)/k_2} k_1 + k_1' \ . \quad (34)$$

The transition-state theory can be used to estimate k_1 in a way similar to the method employed for the CH_3 + CH_3 system [20]:

$$k_1 = Lg_e \frac{RT}{h} \frac{\sum_{j_1} \sum_{k_1} \sum_{j_2} \sum_{k_2} \sum_j \sum_{l=0}^{\langle l_{\text{lim}} \rangle - 1} \sum_J (2J+1) \exp[-E_n(r^{\neq})/RT]}{Q_0} , \quad (35)$$

where

$$Q_0 = \frac{(2\pi\mu RT)^{3/2}}{h^3} \left(\sqrt{\pi \frac{RT}{B_1}} \frac{RT}{A_1} \right)^2 \ . \quad (36)$$

The numerator in Eq. (35) is the statistical sum of the states for the activated complex, [*tert*-$C_4H_9 \cdots$*tert*-C_4H_9]$^{\neq}$, to form *tert*-$C_4H_9 \cdots$*tert*-C_4H_9. As the allowed states for the *tert*-$C_4H_9 \cdots$*tert*-C_4H_9 compounds are only those for which $l < \langle l_{\text{lim}} \rangle$, the sum over l encompasses values in the range from $l = 0$ to $l = \langle l_{\text{lim}} \rangle - 1$. $L = 1/2$ is the ratio of the symmetry coefficients for the reagents and transition state [6, 20]. The factor $g = 1/4$ is the ratio of electronic partition functions as only systems with paired free electrons are usually assumed to be capable of recombination. Ultimately, k_1 can be calculated using the criterion of maximum free energy [2].

As can be seen in Table 2, the values obtained for k_1 are larger by nearly 2 orders of magnitude than the experimental recombination rate constant, $k_{\text{rec},\infty}$, in the high-pressure limit [26]. In the case of methyl radical recombination [20] the reverse situation happened, i.e. $k_1 < k_{\text{rec},\infty}$. Also, the difference between those rate constants is vanishingly small. For instance, for the rate constants given in units of 10^{10} lmol^{-1} s^{-1}, at 823 K $k_1 = 2.15$, while $k_{\text{rec},\infty} = 2.20$ [41]; at 1,350 K $k_1 = 1.68$, while $k_{\text{rec},\infty} = 1.74$ [42]. For these reasons we assumed $k_{\text{rec},\infty} \approx k_1$.

In the present case we have no grounds to assume that $k_{\text{rec},\infty}$ is approximately equal to k_1. Estimates for all the rate constants involved in the mechanism (Eqs. 25, 26, 27, 28, 29, 30, 31, 32) are needed. To this end, we focus our attention on the equilibria that occur in the system investigated.

The equilibrium constant for the reversible reaction

$$\textit{tert}\text{-}C_4H_9 + \textit{tert}\text{-}C_4H_9 \underset{k_{-1}}{\overset{k_1}{\rightleftharpoons}} \textit{tert}\text{-}C_4H_9 \cdots \textit{tert}\text{-}C_4H_9 \quad (37)$$

Table 2. Rate constants k_1, $k_{\text{rec},\infty}$ ($\text{l mol}^{-1}\ \text{s}^{-1}$) and k_{-1}, k_2 (s^{-1})

T/K	k_1	K_{-1}	k_2	$k_{\text{rec},\infty}$ Eq. (68)	Eq. (73)	Exp. [26]
300	7.142×10^{10}	4.436×10^{11}	1.535×10^{10}	2.406×10^{9}	2.472×10^{9}	2.410×10^{9}
400	7.280×10^{10}	7.845×10^{11}	1.625×10^{10}	1.556×10^{9}	1.508×10^{9}	1.565×10^{9}
500	7.259×10^{10}	1.159×10^{12}	1.773×10^{10}	1.123×10^{9}	1.110×10^{9}	1.120×10^{9}
600	7.162×10^{10}	1.554×10^{12}	1.965×10^{10}	8.727×10^{8}	9.055×10^{8}	8.521×10^{8}
800	6.877×10^{10}	2.379×10^{12}	2.458×10^{10}	6.098×10^{8}	7.106×10^{8}	

is given by

$$K_1 = \frac{k_1}{k_{-1}} \ . \tag{38}$$

K_1 can be estimated using the methods of statistical mechanics. Since the radical interactions in a physichemical compound *tert*-$C_4H_9 \cdots$*tert*-C_4H_9 are very weak, the radicals can be assumed to retain their individual properties. If so, the enthalpies of formation for the *tert*-C_4H_9 in the reactants and products can be assumed as equal. Using this assumption we obtain

$$K_1 = N_A g_e \frac{h^3}{(2\pi\mu RT)^{3/2}} \frac{Q_{C_4H_9 \cdots C_4H_9}}{Q_{C_4H_9} Q_{C_4H_9}} \ . \tag{39}$$

N_A is the Avogadro number and $Q_{C_4H_9} = Q^{\text{rot}}_{C_4H_9} Q^{\text{osc}}_{C_4H_9}$ is the statistical sum for *tert*-C_4H_9 which takes into account rotational and vibrational degrees of freedom. The sums are estimated using standard methods [39, 43]. Since vibrational frequencies for *tert*-C_4H_9 are not known, the vibrational frequencies for isobutane [35] were used by rejecting three vibrations of a hydrogen linked to the central carbon atom. Thus, the vibrational frequencies (reciprocal centimetres) for *tert*-C_4H_9 are 2,962(6), 2,906, 2,894(2), 1,477(3), 1,475(3), 1,394, 1,371(2), 1,177, 1,166(2), 966(3), 918(2), 797, 426, 367(2) and 198(3). The symmetry coefficient for the rigid *tert*-butyl radical is 6. Taking into account the internal rotations leads to a total symmetry number of 6×3^3.

The statistical sum for the unstable *tert*-$C_4H_9 \cdots$*tert*-C_4H_9 compounds, $Q_{C_4H_9 \cdots C_4H_9}$, can be estimated using the E_v vibrational levels, Eq. (24). The orbital energy was not taken into account when calculating such levels. Thus, the effect of orbital motion on the vibrational levels is neglected. However, by writing this part of energy in the form of Eq. (40), the coupling of rotational and vibrational motion is accounted for [43, 44]:

$$E_{v,l} = E_v + B_v l(l+1) - D l^2 (l+1)^2 \ , \tag{40}$$

where

$$B_v = B - \alpha\left(v + \frac{1}{2}\right) \ , \tag{41}$$

$$B = \frac{\hbar^2}{2\mu r^2} \tag{42}$$

$$D = \frac{4B^3}{(h\nu_0)^2} \tag{43}$$

and

$$\alpha = \frac{6B^2}{h\nu_0}\left[\left(\frac{xh\nu_0}{B}\right)^{\frac{1}{2}} - 1\right] \ . \tag{44}$$

Using these equations the statistical sum of the orbital and vibrational motion along r is obtained in the form

$$Q_{\text{vib,orb}} = \sum_{l=0}^{\langle l_{\lim}\rangle - 1} \sum_{v=0}^{v_{\max}} (2l+1) \exp(-E_{v,l}/RT) \ , \tag{45}$$

where $v_{\max} = 17$. For any given l, the depth and location of the minimum on the $E_n(r)$ curve were examined. The well depth decreases as l increases (Fig. 1). For this reason only those components of the sum (Eq. 45) are included that feature $E_{v,l}$ smaller than the maximum on the $E_n(r)$ curve. For large orbital momenta, $l > 190$, the bonded state is, as a rule, represented by only one, the lowest, vibrational state ($v = 0$). To assess the accuracy of the approximation to the sum, $Q_{C_4H_9 \cdots C_4H_9}$ the change in $h\nu_0$ within reasonable limits can be used. We estimated in this way that the result can be in error by no more than a factor of 1.5. Ultimately, we obtain

$$Q_{C_4H_9 \cdots C_4H_9} = \left(Q^{\text{rot}}_{C_4H_9} Q^{\text{osc}}_{C_4H_9}\right)^2 Q_{\text{vib,orb}} \ . \tag{46}$$

The symmetry coefficient associated with external rotations, by analogy to the $CH_3 + CH_3$ system [6, 20], is assumed to be 72. If internal rotations are accounted for, the total symmetry number increases to 72×3^6.

Next we consider the equilibrium

$$tert{-}C_4H_9 \cdots tert{-}C_4H_9 \underset{k_{-2}}{\overset{k_2}{\rightleftharpoons}} C_8H_{18}^* \ . \tag{47}$$

The equilibrium constant is given by

$$K_2 = \frac{k_2}{k_{-2}} \tag{48}$$

and

$$K_2 = \frac{Q_{C_8H_{18}}}{Q_{C_4H_9 \cdots C_4H_9}} \exp\left(\Delta H_0^0/RT\right) \ , \tag{49}$$

where $\Delta H_0{}^0$ is the enthalpy for the rupture of the C–C bond at 0 K. It is estimated on the basis of the enthalpy of formation: $\Delta H_f(C_8H_{18}) = -53.92\ \text{kcal mol}^{-1}$ [45] and $\Delta H_f(tert\text{-}C_4H_9) = 13.145\ \text{kcal mol}^{-1}$ [46]. On the basis of the usual assumption that the differences in the enthalpies of formation at room temperature and 0 K are slight $\Delta H_0{}^0 = 80.21\ \text{kcal mol}^{-1}$ is obtained. $Q_{C_8H_{18}}$ is the statistical sum for C_8H_{18} which takes into account rotational and vibrational degrees of freedom. The vibrational frequencies (reciprocal centimetres) for tetramethylbutane are [47] 2,962, 2,959(2), 2,964(4), 2,963, 2,883, 2,961(4), 2,882(5), 1,478, 1,459(2), 1,467(2), 1,464(3), 1,458(4), 1,380, 1,392(2), 1,370, 1,373(2), 1,322, 1,262(2), 1,206, 1,222(2), 1,018(2), 1,008(2), 981(2), 918(2), 931(2), 883, 797, 652, 480(2), 464, 384(2), 329(2), 282, 226(2), 200(2), 199, 198, 188(2) and 48. The symmetry number for tetramethylbutane taking into account internal rotations is $6 \times 3 \times 3^6$. On the basis of the geometrical parameters for alkanes [35], the rotational constants are $A_0 = B_0 = 1.70 \times 10^{-4}$ kcal mol^{-1} and $C_0 = 2.22 \times 10^{-4}$ kcal mol^{-1}.

We also consider the equilibrium

$$\text{tert-}C_4H_9 + \text{tert-}C_4H_9 \underset{k_{-3}}{\overset{k_3}{\rightleftharpoons}} C_8H_{18}^* \ , \tag{50}$$

where

$$K_3 = \frac{k_3}{k_{-3}} \tag{51}$$

and

$$K_3 = N_A g_\mathrm{e} \frac{h^3}{(2\pi\mu RT)^{3/2}} \frac{Q_{\mathrm{C_8H_{18}}}}{Q_{\mathrm{C_4H_9}} Q_{\mathrm{C_4H_9}}} \exp\left(\Delta H_0^0/RT\right) \ . \tag{52}$$

Equation (50) does not account for any specific mechanisms. The meaning of the symbols is the same as before.

4 Correlation of the reactant and product states

The constants k_1 and $k_{-1} = k_1/K_1$ (Table 2) were calculated on the basis of the known energy of radical interactions and solutions of the Schrödinger equations (Eqs. 11, 16). Estimation of k_2 and k_{-2} presents more difficulties. Equation (50) involves the transfer from loosely to strongly bonded states and vice versa. The details of such a transfer are unknown even for such a widely studied model system as CH_3 + CH_3. The theories that correlate the initial states of the reactants with the final states of the products can be helpful. The canonical and microcanonical model developed originally by Quack and Troe [1, 48] and another microcanonical model created by Forst [49], using a Laplace transform of his own model, yielded very reasonable results for the CH_3 + H and CH_3 + CH_3 systems [49]. Both theories [48, 49] will be used to estimate k_2 and k_{-2}.

The original formulations of the theory were modified to a slight extent using the fact that Eq. (47) exhibits some features of isomerization. k_{-2} is written in the form

$$k_{-2} = \frac{RT}{h} \frac{Q_{\mathrm{el}}(r) Q_\mathrm{c}(r) Q^z_{\mathrm{vr}}(r)}{Q^z_{\mathrm{C_8H_{18}}}} \ . \tag{53}$$

The value for k_{-2} is selected at $r = r^{\neq}$ determined using a criterion of maximum free energy [2]. The meaning of the symbols is as follows.

$$Q_{\mathrm{el}}(r) = \exp\left(-D_\mathrm{e}\{1 - \exp[-\beta_\mathrm{e}(r - r_\mathrm{e})]\}^2/RT\right) \tag{54}$$

is the contribution of electronic energy represented by the Morse function along the C–C bond which is the reaction coordinate with $r_\mathrm{e} = 1.525$ Å. On the basis of $\Delta H_0{}^0$ and the vibrational frequencies estimated earlier, using the standard methods we obtain $D_\mathrm{e} = 83.81$ kcal mol^{-1} and $\beta_\mathrm{e} = 1.93$ Å^{-1}.

$Q_\mathrm{c}(r)$ is the centrifugal partition function:

$$Q_\mathrm{c}(r) = \frac{2\mu r^2 RT}{\hbar^2} \ . \tag{55}$$

$Q^z{}_{\mathrm{vr}}(r)$ is the statistical sum of vibrational–rotational states of the transition complex. The superscript z denotes the inclusion of the oscillation energy of the lowest vibrational state. The rovibrational statistical sum of states over the substrate region, i.e. at $r = r_\mathrm{e}$, is denoted $Q^z{}_{\mathrm{vr}}$(subs). The statistical sum of rovibrational states over the product region, i.e. at $r = r_0$, is denoted $Q^z{}_{\mathrm{vr}}$(prod).

$Q^z{}_{\mathrm{vr}}$(subs) accounts for the rovibrational states of C_8H_{18} excluding stretching vibrations along the C–C bond ($h\nu_{\mathrm{RC}} = 652$ cm^{-1}). In simple dissociations this degree of freedom becomes, over the product region, translation along the reaction coordinate. Our case is more involved. An occurrence of slow vibrations, $h\nu_0 = 42.7$ cm^{-1}, can be assumed. These vibrations have to be eliminated from $Q^z{}_{\mathrm{vr}}$(prod). Thus, the most convenient way to estimate $Q^z{}_{\mathrm{vr}}$(subs) and $Q^z{}_{\mathrm{vr}}$(prod) is as follows. Let the sum of stretching vibrations $h\nu_{\mathrm{RC}}$ be

$$Q^z_{\mathrm{RC}} = \frac{\exp\left(-\frac{1}{2}h\nu_{\mathrm{RC}}/RT\right)}{1 - \exp(-h\nu_{\mathrm{RC}}/RT)} \ . \tag{56}$$

Then, the sum of the vibrational–rotational states of the system in the region of substrates is given by

$$Q^z_{\mathrm{vr}}(\mathrm{subs}) = \frac{Q^z_{\mathrm{C_8H_{18}}}}{Q^z_{\mathrm{RC}} Q_\mathrm{c}(r_\mathrm{e})} \ , \tag{57}$$

where $Q^z_{\mathrm{C_8H_{18}}}$ is the sum of vibrational and rotational states for C_8H_{18} accounting for the zero-order frequencies and the total symmetry number. Calculation of $Q^z{}_{\mathrm{vr}}$(prod) follows the same rules. The statistical sum of the vibrations with $h\nu_0$ is given by

$$Q'^z_{\mathrm{RC}} = \sum_{v=0}^{v_{\max}} \exp\left\{-\left[h\nu_0\left(v + \frac{1}{2}\right) - xh\nu_0\left(v + \frac{1}{2}\right)^2\right] \Big/ RT\right\} \ . \tag{58}$$

Estimation of the centrifugal partition function in the product region takes into account the dependence of the location of equilibrium $r_0{}'$ on the orbital number l, (Fig. 1), and the limited number of available orbital states ($l < \langle l_{\lim}\rangle$):

$$Q'_\mathrm{c} = \sum_{l=0}^{\langle l_{\lim}\rangle - 1} (2l + 1) \exp\left(-\frac{\hbar^2}{2\mu r_0'^2 RT} l(l + 1)\right) \ . \tag{59}$$

Accordingly

$$Q^z_{\mathrm{vr}}(\mathrm{prod}) = \frac{Q^z_{\mathrm{C_4H_9 \cdots C_4H_9}}}{Q'^z_{\mathrm{RC}} Q'_\mathrm{c}} \ , \tag{60}$$

where $Q^{z}_{C_4H_9 \cdots C_4H_9}$ is the statistical sum of the vibrational and rotational states of *tert*-$C_4H_9 \cdots$*tert*-C_4H_9 compounds accounting for the zero-order vibrations and the total symmetry number (cf. Eq. 46).

According to the theory used here, $Q^{z}{}_{vr}(r)$ is estimated from

$$\ln Q^{z}_{vr}(r) = \left[\ln Q^{z}_{vr}(\mathrm{subs}) - \ln Q^{z}_{vr}(\mathrm{prod})\right] S(r) + \ln Q^{z}_{vr}(\mathrm{prod}) \ . \tag{61}$$

The $S(r)$ switching function deserves a few words of comment. There are a number of options [48, 49] from which we have chosen the two-parameter hyperbolic tangent function [49]:

$$S(r) = 1 - \tanh\left[a(r - r_e)^{b}\right] \ , \tag{62}$$

where a and b are the parameters to be fitted. This function has to be modified so that the $Q^{z}{}_{vr}(r)$ sum obeys the conditions $Q^{z}{}_{vr}(r \rightarrow r_e) = Q^{z}{}_{vr}(\mathrm{subs})$ and $Q^{z}{}_{vr}(r \rightarrow r_0) = Q^{z}{}_{vr}(\mathrm{prod})$. Over the range $r_e < r < r_0$ we postulate the following form for the switching function:

$$S(r) = 1 - \tanh\left[a\left(\frac{r - r_e}{r_0 - r}\right)^{b}\right] \ . \tag{63}$$

Ultimately, the rate constant (Eq. 53) is calculated by minimization with respect to r, which is equivalent to the use of the previously mentioned criterion of maximum free energy. The best agreement with experiment [26] is obtained for the parameters $a = 0.6412$ and $b = 0.4809$. Some examples for $k_2 = k_{-2}K_2$ are listed in Table 2.

5 The final form for $k_{\mathrm{rec},\infty}(T)$

The calculations indicate that the rates for Eqs. (26) and (28) obey the relation (Table 2)

$$\frac{k_{-1}}{k_2} \gg 1 \ . \tag{64}$$

Moreover, over the large range of temperatures $T > 300$ K and at high pressures (up to about 100 atm in the presence of different bath gases) the following inequality is obeyed:

$$k_{-1} > \lambda Z p \ . \tag{65}$$

These relations, combined with Eq. (34) for the recombination rate constant at high pressures, lead to the approximate relation:

$$k_{\mathrm{rec},\infty} \approx K_1 k_2 + k'_1 \ . \tag{66}$$

$k_1{}'$ refers to the recombinations that occur at the initial condition $l > \langle l_{\mathrm{lim}} \rangle$. Even though the exact mechanism is unknown, a reasonable assessment of the contribution of such processes to the overall recombination can be made. Consider k_{-3} (Eq. 50) as the overall recombination rate constant ignoring intermediate reaction pathways. Note that except for our work, this is an approach used in all the work concerned with $CH_3 + CH_3$ and $CH_3 + H$ recombinations cited in the Introduction. k_{-3} can be estimated by using the theory described earlier; only the switching function (Eq. 63) is replaced by Eq. (62) and Eq. (60) is replaced by

$$Q^{z}_{vr}(prod) = Q^{z}_{C_4H_9} Q^{z}_{C_4H_9} \ , \tag{67}$$

where $Q^{z}_{C_4H_9}$ is the statistical sum for *tert*-C_4H_9 which takes into account rotational and vibrational degrees of freedom, including the zero-order vibrations and the full symmetry number. Using the procedure described previously the best agreement of $k_{\mathrm{rec},\infty} \approx k_3 = k_{-3}K_3$ with experiment [26] was obtained at $a = 0.1321$ Å^{-2} and $b = 2$. Since this result for $k_{\mathrm{rec},\infty} \approx k_3$ seems to be acceptable (Table 2), we represent the overall recombination rate constant as the sum

$$k_{\mathrm{rec},\infty} \approx \sum_{l=0}^{\langle l_{\mathrm{lim}} \rangle - 1} k_3(l) P(l) + \sum_{l=\langle l_{\mathrm{lim}} \rangle}^{l=\infty} k_3(l) P(l) \ , \tag{68}$$

where

$$k_3(l) = \frac{RT}{h} \frac{Q_{\mathrm{el}}(r) Q^{z}_{vr}(r)}{Q^{z}_{C_8H_{18}}} \exp\left(-\frac{E_l(r)}{RT}\right) K_3 \ , \tag{69}$$

$$E_l(r) = l(l+1)\frac{\hbar^2}{2\mu r^2} - l(l+1)\frac{\hbar^2}{2\mu r_e^2} \tag{70}$$

and

$$P(l) = (2l+1)\exp\left(-l(l+1)\frac{\hbar^2}{2RT\mu r_e^2}\right) \ . \tag{71}$$

A comparison of Eqs. (66) and (68) indicates that the first term in Eq. (68) represents contributions stemming from the initial condition $l < \langle l_{\mathrm{lim}} \rangle$, whereas the second term represents those stemming from the condition $l > \langle l_{\mathrm{lim}} \rangle$. The ratio of the second term to the first yields about 3×10^{-5} at 300 K, about 9×10^{-4} at 500 K, and increases up to about 2×10^{-3} at 600 K. It can be estimated that the contributions to $k_{\mathrm{rec},\infty}$ from the states with $l > \langle l_{\mathrm{lim}} \rangle$, $k_1{}'$, are smaller by 3 orders of magnitude than those involving states with $l < \langle l_{\mathrm{lim}} \rangle$. More sophisticated calculations using the microcanonical model are unlikely to alter this assessment [49]. Thus, the contribution from $k_1{}'$ can be safely ignored, which leads to

$$k_{\mathrm{rec},\infty} \approx K_1 k_2 \ . \tag{72}$$

Using the definitions derived earlier leads to the final recombination rate constants for *tert*-butyl radicals in the form

$$k_{\mathrm{rec},\infty} \approx N_A L g_e \left(\frac{h}{RT}\right)^{3/2} \left(\frac{h}{2\pi\mu}\right)^{3/2} k_2 Q_{\mathrm{vib,orb}} \ , \tag{73}$$

where $L = 1/2$ is the ratio of the symmetry numbers of the reactants and the transient *tert*-$C_4H_9 \cdots$*tert*-C_4H_9. Since over the range 300 K $< T <$ 600 K, $k_2 Q_{\mathrm{vib,orb}}$ is very weakly dependent on temperature (Table 3), the recombination rate constants for *tert*-butyl radicals obey the proportionality $k_{\mathrm{rec},\infty} \sim T^{-3/2}$.

Table 3. Equilibrium rate constants and statistical sum $Q_{\mathrm{vib,orb}}$ for the physicochemical compounds *tert*-C_4H_9...*tert*-C_4H_9

T/K	K_2	$K_3/(\mathrm{lmol}^{-1})$	$Q_{\mathrm{vib,orb}}$	$k_2Q_{\mathrm{vib,orb}} \times \mathrm{s}$
300	6.366×10^{50}	1.031×10^{50}	3.175×10^{5}	4.875×10^{15}
400	2.716×10^{36}	2.535×10^{35}	2.817×10^{5}	4.578×10^{15}
500	7.546×10^{27}	4.752×10^{26}	2.657×10^{5}	4.711×10^{15}
600	1.669×10^{22}	7.735×10^{20}	2.570×10^{5}	5.051×10^{15}
800	1.774×10^{15}	5.156×10^{13}	2.482×10^{5}	6.103×10^{15}

6 Discussion and conclusions

The successes of the variational version of transition-state theory [5, 6, 10, 11], exemplified above all by the works of Wardlaw, led to the explanation of the negative temperature dependences of the recombination rate constants. This explanation can be summarized as follows. As the temperature increases the location of the transition state, $r^{\neq}$, shifts towards smaller distances. At such small distances, for example, $r = 3.37$ Å at 1,000 K for the CH_3 + CH_3 system [11], short-range, strong interactions, especially of the V_{NB} type, predominate. The canonical version of flexible transition-state theory shows substantial variations of $k_{\mathrm{rec},\infty}$ with this potential, with limits set by the free rotor and harmonic oscillator behaviour of the angular modes. As the V_{NB} potential, particularly in the repulsive region, becomes more significant, the negative temperature dependence becomes much stronger (e.g. $CH_3 + H$ versus CH_3 + CH_3 versus *tert*-C_4H_9 + *tert*-C_4H_9).

Although such an explanation certainly contains a grain of truth, it still seems to be oversimplified and rather misleading. In fundamental definitions used for the estimations of reaction rate constants, such as the method of classical trajectories [50, 51] or the fundamental formulation of SACM [1], the idea of a transition state located at a distance $r^{\neq}$ is not indispensable. It gains importance only after some simplification has been assumed: neglect of the equations of motion for the transfer from reactants to products. The mechanisms postulated in our works include to some extent such solutions.

In the CH_3 + CH_3 system, the $CH_3 \cdots CH_3$ transients are formed with a rate constant k_1 and yield subsequently $C_2H_6^{\ast}$ with a rate constant k_2 [20]. The latter process is much faster than the spontaneous dissociation of $CH_3 \cdots CH_3$ back to reactants, $k_2 > > k_{-1}$. For this reason $k_{\mathrm{rec},\infty}$ is limited by k_1, which depends on temperature as $T^{-1/2}$.

The mechanism for *tert*-butyl recombination is more involved. The *tert*-$C_4H_9\cdots$*tert*-C_4H_9 transients are formed readily as is evidenced by the large value for k_1. In this case, however, the recombination is much slower than the spontaneous decomposition *tert*-$C_4H_9\cdots$*tert*-C_4H_9 back into reactants, $k_2 \ll k_{-1}$. The steric effects due to the presence of methyl groups that substitute hydrogen atoms may offer an explanation. The effective overlap of the shells with a vacancy is now more difficult. The methyl groups augment the V_{NB} potential and a rate-determining minimum is shifted to distances exceeding 5 Å. It is reasonable to assume that the bonded interactions are negligible at such large distances.

The steric hindrance between the fragments is likely to be a major reason for the strong negative temperature dependence. The problem is worthy of further investigation.

Both k_2 and the equilibrium constant K_1 affect the rate for recombination in the *tert*-C_4H_9 + *tert*-C_4H_9 system, $k_{\mathrm{rec},\infty} \approx K_1k_2$. Since over the range 300–600 K k_2 exhibits a weak temperature dependence (Table 2), the temperature dependence for the recombination of *tert*-butyl radicals depends mostly on K_1. If correct, it means that for both methyl and *tert*-butyl radicals the temperature dependence of the recombination rate constant is determined by k_1 and k_{-1}. Weak, long-range van der Waals interactions rather than strong, short range interactions seem to be of paramount importance.

This is not so in the case of CH_3 + H recombination, which exhibits the smallest contribution of van der Waals interactions ($\langle l_{\mathrm{lim}}\rangle = 13$). Experiments indicate that direct recombination, not involving loosely bonded transients, plays a major role, leading to a large value for $k_1{}'$. The superposition $k_{\mathrm{rec},\infty} \approx k_1 + k_1{}'$ determines the temperature dependence. The final result may also be pseudoindependent of temperature [21].

Acknowledgements. We thank the anonymous referees for their helpful comments.

References

1. Quack M, Troe J (1974) Ber Bunsenges Phys Chem 78: 240
2. Hase WL (1983) Acc Chem Res 16: 258
3. Hase WL, Mondro SL, Duchovic RJ, Hirst DM (1987) J Am Chem Soc 109: 2916
4. Hu X, Hase WL (1989) J Phys Chem 93: 6029
5. Aubanel EE, Wardlaw DM (1989) J Phys Chem 93: 3117
6. Wardlaw DM, Marcus RA (1986) J Phys Chem 90: 5383
7. Klippenstein SJ, Marcus RA (1987) J Chem Phys 87: 3410
8. Wagner AF, Wardlaw DM (1988) J Phys Chem 92: 2462
9. Darvesh KV, Boyd RJ, Pacey PD (1989) J Phys Chem 93: 4772
10. Robertson SH, Wardlaw DM, Hirst DM (1993) J Chem Phys 99: 7748
11. Pesa M, Pilling MJ, Robertson SH, Wardlaw DM (1998) J Phys Chem A 102: 8526
12. Klippenstein SJ, Harding LB (1999) J Phys Chem A 103: 9388
13. Hu X, Hase WL (1991) J Chem Phys 95: 8073
14. Gorin E (1939) J Chem Phys 7: 256
15. Benson SW (1983) Can J Chem 61: 881
16. Pitt IG, Gilbert RG, Ryan KR (1995) J Phys Chem 99: 239
17. Pacey PD (1998) J Phys Chem A 102: 8541
18. Naroznik M, Niedzielski J (1996) Theor Chim Acta 94: 257
19. Naroznik M, Niedzielski J (1996) Theor Chim Acta 94: 271
20. Naroznik M (1998) J Chem Soc Faraday Trans 94: 2531
21. Naroznik M, Niedzielski J (1998) J Chem Soc Faraday Trans 94: 2541
22. Clary DC (1984) Mol Phys 53: 3
23. Metcalfe EL (1963) J Chem Soc 3560
24. Hiatt R, Benson SW (1973) Int J Chem Kinet 5: 385
25. Choo KY, Beadle PC, Piszkiewicz LW, Golden DM (1976) Int J Chem Kinet 8: 45
26. Parkes DA, Quinn CP (1976) J Chem Soc Faraday Trans 172: 1952
27. Bethune DS, Lankard JR, Sorokin PP, Schell-Sorokin AJ, Plecnik RM, Avouris P (1981) J Chem Phys 75: 2231

28. Kerr JA, Moss SJ (1981) CRC handbook of bimolecular and termolecular gas reactions. vol II. CRC, Boca Raton
29. Pilling M (1996) Annu Rev Phys Chem 47: 81
30. Murrell JN, Carter S, Farantos SC, Huxley P, Varandas AJC, (1984) Molecular potential energy functions. Wiley, Chichester
31. Kihara T (1970) In: Eyring H, Henderson D, Jost W (eds) Physical chemistry, an advanced treatise, vol V. Academic, New York, pp
32. Stone AJ (1996) The theory of intermolecular forces, Clarendon, Oxford
33. Strein K, Lichtenhaler RN, Schlafer KL (1971) Ber Bunsen-Ges 75: 1308
34. Naroznik M to be published
35. Swerdlov LM, Kovner MA, Krainov EP (1970) Vibrational spectra of polyatomic molecules (in Russian). Moscow
36. Warshalovitsch DA, Moskalev AN, Khersonsky WK (1975) Quantum theory of the angular momentum (in Russian). Nauka, Leningrad
37. Brojan JB, Mostowski J, Wodkiewicz K (1976) Problems in quantum mechanics (in Polish). PWN, Warsaw
38. Slagle IR, Gutman D, Davies JW, Pilling MJ (1988) J Phys Chem 92: 2455
39. Robinson PJ, Holbrook KA (1972) Unimolecular reactions. Wiley-Interscience, London
40. Forst W (1973) Theory of unimolecular reactions, Academic, New York
41. Pacey PD, Wimalasena JH (1980) J Phys Chem 84: 2221
42. Glanzer K, Quack M, Troe J (1976) Chem Phys Lett 39: 304
43. Smirnova NA (1980) Methods of statistical thermodynamics in physical chemistry (in Polish). PWN, Warsaw
44. Herzberg G (1966) Molecular spectra and molecular structure, vol 3. Van Nostrand Reinhold, New York
45. Lide DR (1992–1993) (ed) Handbook of chemistry and physics, 73rd edn. CRC, Boca Raton
46. Smith BJ, Radom L (1998) J Phys Chem 102: 10787
47. Snyder RG, Schachtschneider JH (1965) Spectrochim Acta 21: 169
48. Quack M, Troe J (1977) Ber Bunsenges Phys Chem 81: 329
49. Forst W (1991) J Phys Chem 95: 3612
50. Miller WH (1974) J Chem Phys 61: 1823
51. Su T, Chesnavich WJ (1982) J Chem Phys 76: 5183